

# Time-reversed information flow through a wormhole in scalar–tensor gravity

Hoang Ky Nguyen\*

*Department of Physics, Babeş–Bolyai University, Cluj-Napoca 400084, Romania*

Francisco S. N. Lobo†

*Instituto de Astrofísica e Ciências do Espaço, Faculdade de Ciências da Universidade de Lisboa, Campo Grande, Edifício C8, P-1749-016 Lisbon, Portugal and*

*Departamento de Física, Faculdade de Ciências da Universidade de Lisboa, Campo Grande, Edifício C8, P-1749-016 Lisbon, Portugal*

(Dated: July 2, 2024)

This Letter aims to advance unexplored properties of a new class of Closed Timelike Curves recently discovered in scalar–tensor gravity, reported in [Universe 9, 467 \(2023\)](#) and [Eur. Phys. J. C 83, 626 \(2023\)](#). Therein, it was shown that when the Weak Energy Condition is violated, the topology of spacetime in scalar–tensor gravity is altered, enabling the formation of two-way traversable wormholes. Furthermore, each of these wormholes acts a gateway between two *time-mirrored* worlds, where the two asymptotically flat sheets in the Kruskal–Szekeres diagram are glued antipodally along *three* directions—time  $t$  and the polar and azimuth angles  $(\theta, \varphi)$  of the 2-sphere—to form a wormhole throat. This contrasts with the standard embedding diagram which typically glues the sheets only along the  $\theta$  and  $\varphi$  directions. Crucially, due to the ‘gluing’ along the  $t$  direction, the wormhole becomes a portal connecting the two spacetime sheets with *opposite* physical time flows, enabling the emergence of closed timelike loops which straddle the throat. In this Letter, we shall point out that this portal *mathematically* permits the possibility of backward propagation of information *against* time. This feature is ubiquitous for wormholes in scalar–tensor theories. In addition, we formulate the Feynman sum for transition amplitudes of microscopic particles in the proximity of a wormhole throat in which we account for timelike paths that experience time reversal.

*Introduction*—Closed timelike curves (CTCs) are mathematical constructs first emerging in the context of General Relativity via the pioneering works of van Stockum and Gödel [1, 2]. These curves represent paths through spacetime that loop back on themselves, allowing an object or observer to return to an event in its own past. Interests in CTCs were revived in the works of Thorne and Novikov in the context of the Morris–Thorne wormholes which are thought to occur in the presence of exotic matter (or in modified gravity) [3–8]. Despite the problematic nature of CTCs, the mathematical validity sparked considerable interest among gravitational theorists [9–19]. The concept of CTCs serves as a “gedanken experiment”, compelling us to grapple with and reevaluate the foundational principles of general relativity and its modifications.

Soon after the works of Thorne and collaborators, Deutsch and Politzer attempted to investigate quantum effects associated with CTCs. They introduced the Deutsch–Politzer (DP) space—an abstract construct created through surgical manipulation on a two-dimensional Lorentzian spacetime, forming a cylinder-shaped ‘handle’ that bridges two spacelike regions [20–23]. This process is visually depicted in Fig. 1, where Paths 3 and 4 represent CTCs. As an object moves along a CTC, proper time continues to cumulate (i.e., the time count registered by a clock carried along the path keeps increasing),

but the object eventually returns to its original spacetime point. Whereas geometry pertains to local properties of spacetime, topology pertains to global ones; in crafting a ‘handle’, the DP surgery deliberately alters the *topology* of spacetime, allowing for CTCs to emerge.

While DP space, as a conceptual model, serves its purpose, it is preferable to *derive* alterations to spacetime topology from a concrete theory of gravity. In fact, in General Relativity, it was shown that through the Einstein field equations these spacetimes violate the Weak Energy Condition (WEC) [3]. Matter that violates the WEC is denoted *exotic matter*, and can spontaneously induce spacetime to acquire non-trivial topologies, such as the Morris–Thorne wormholes that facilitates CTCs [4, 5, 8, 24, 25].

In a series of recent papers [26–28], one of the authors extended Buchdahl’s work in pure  $\mathcal{R}^2$  gravity [29], culminating in a static spherically symmetric vacuum solution. Notably, despite the absence of exotic matter, the higher-derivative terms in the theory formally violate the WEC, under certain conditions. This violation enables the construction of a two-way traversable wormhole, which we named the Morris–Thorne–Buchdahl (MTB) wormhole [30]. Importantly, the analytical solution has allowed us to construct a  $(\zeta-)$ Kruskal–Szekeres (KS) diagram, revealing a non-trivial topology. The  $(\zeta-)$ KS coordinates enable for an identification procedure that results in the wormhole throat bridging two asymptotically flat spacetime sheets with opposing flows of proper time, as we recently proposed in [31]. Physical processes occurring

\* hoang.nguyen@ubbcluj.ro

† fslolo@fc.ul.pt

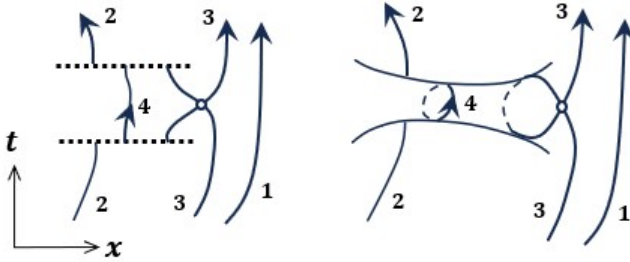


Figure 1. The Deutsch–Politzer surgery. In the left panel, a 2-dimensional Minkowski spacetime is incised along the two dotted segments. The banks of the cuts are then glued together to form a ‘handle’, as shown in the right panel. Paths 1 and 2 represent regular trajectories in Minkowski spacetime. Path 3 is self-crossing, resulting in a portion of it forming a closed timelike curve (CTC). Path 4 depicts an infinite loop.

in the two spacetime sheets across the throat evolve in opposite time directions. In essence, the MTB wormhole throat serves as a “gateway to another *time-reversed* world”. More generally, we have found that this property is a universal feature for Brans–Dicke and scalar–tensor gravities [32]. It is important to note that embedding diagrams, a standard tool to visualize wormholes, are *inadequate* in exposing this feature, as we shall explain in a later section of this Letter.

Importantly, the construction of the CTC that we presented in [31] *does not necessitate one wormhole mouth to move at high speed or be situated near a supermassive object to accumulate time dilation*—a procedure commonly portrayed in the literature [4, 8]. The resulting CTC is of a novel type, offering intriguing avenues for exploration and analysis.

*The special Buchdahl-inspired metric*—Consider the vacuum pure  $\mathcal{R}^2$  field equation [26]

$$\mathcal{R} \left( \mathcal{R}_{\mu\nu} - \frac{1}{4} g_{\mu\nu} \mathcal{R} \right) + g_{\mu\nu} \square \mathcal{R} - \nabla_\mu \nabla_\nu \mathcal{R} = 0 \quad (1)$$

Among a variety of solutions [27, 32], the *asymptotically flat* Buchdahl-inspired solution to Eq. (1) expressed in the KS coordinates is given by [26]

$$ds^2 = -4e^{-r^*(r)} \left(1 - \frac{r_s}{r}\right)^{\frac{\tilde{k}+1}{\zeta}} (dT^2 - dX^2) + \left(1 - \frac{r_s}{r}\right)^{\frac{\zeta+\tilde{k}-1}{\zeta}} r^2 d\Omega^2 \quad (2)$$

and

$$T^2 - X^2 = -e^{r^*(r)}; \quad \frac{T}{X} = \tanh \frac{t}{2r_s} \quad (3)$$

which depend on a dimensionless (Buchdahl) parameter  $\tilde{k}$ , and  $\zeta := (1 + 3\tilde{k}^2)^{1/2}$ , whereas the tortoise coordinate  $r^*(r)$  involves a Gaussian hypergeometric function and is given in [26]. Note: per Eqs. (3), each pair of coordinates  $(t, r)$  corresponds to *two* pairs of KS coordinates  $(T, X)$  and  $(-T, -X)$ .

In Ref. [30] we showed that, for  $\tilde{k} \in (-1, 0)$ , the WEC is formally violated. Simultaneously, the areal radius,  $R(r) =$

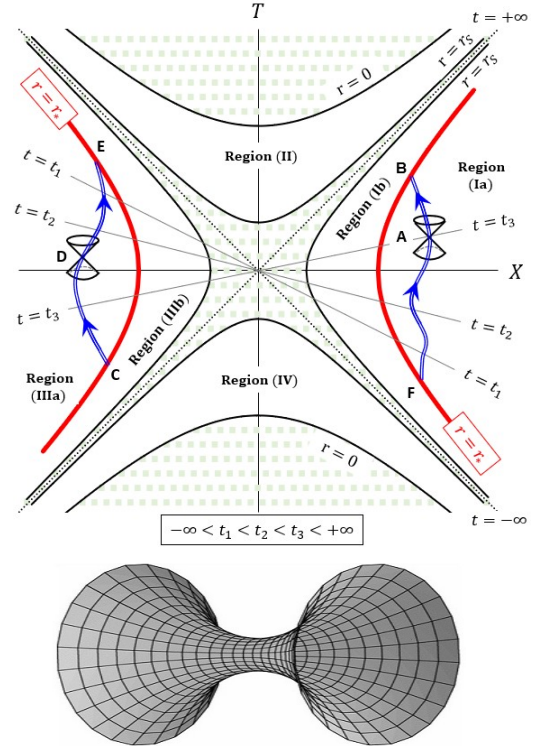


Figure 2. Visualizing a Buchdahl-inspired spacetime. While the embedding diagram (lower panel) suggests ‘gluing’ at a fixed timeslice  $T$ , the  $\zeta$ –KS diagram (upper panel) makes the ‘gluing’ along the *time* direction, with the two thick red lines are identical *antipodally*. An MTB wormhole is formed by flipping Region (IIIa) upside down and gluing it with Region (Ia). Trajectory (ABCDEFA) forms a closed timelike loop.

$$r \left(1 - \frac{r_s}{r}\right)^{\frac{\zeta+\tilde{k}-1}{2\zeta}}, \text{ attains a (local) minimum at} \\ r_* = \frac{\zeta - \tilde{k} + 1}{2\zeta} r_s \quad (4)$$

which exceeds  $r_s$  when  $\tilde{k} \in (-1, 0)$ . In this scenario, the spacetime forms a two-way traversable wormhole, referred to as the MTB wormhole, with its throat located at  $r_*$  given in (4), to be briefly described below. An embedding diagram is shown in Fig. 2.

Restricting within the  $(T, X)$  plane (viz.  $d\theta = d\varphi = 0$ ), the  $\zeta$ –KS diagram for the metric (2)–(3) is shown in Fig. 2. The diagram is self-explanatory [30]: (i) It is conformally Minkowski, with null geodesics being  $dX = \pm dT$ . (ii) A constant- $t$  contour corresponds to a straight line running through the origin of the  $(T, X)$  plane. (iii) Regions (I) and (III) are mirror images of each other, upon flipping the sign of the KS coordinates, viz.  $(T, X) \leftrightarrow (-T, -X)$ . (iv) For  $\tilde{k} \in (-1, 0)$ , the hyperbola  $r = r_*$  (thick red lines) splits these regions into sub-regions (Ia), (Ib), (IIIa), (IIIb). The ‘outer’ sub-regions (Ia) and (IIIa) are asymptotically flat spacetime sheets which are devoid of physical singularities.

*Identification of antipodal points and emergence of CTCs*—Antipodal points play a crucial role in the  $\zeta$ –KS diagram. Specifically, the two thick red lines on the diagram, in Fig. 2,

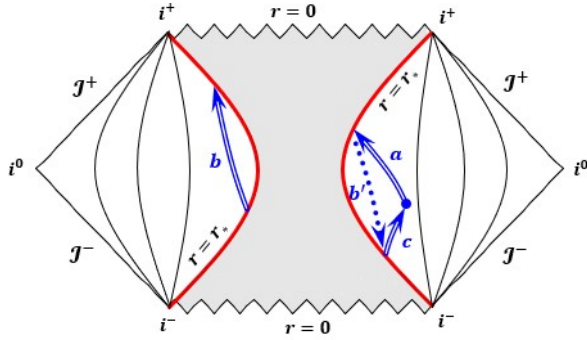


Figure 3. Penrose diagram illustrating an MTB wormhole with its two sheets presented as the left and right wedges. Constant- $r$  contours connecting  $i^-$  with  $i^+$  are shown. The wedges are glued along the thick red lines, corresponding to the throat at  $r = r_*$ , but with the left wedge and line flipped upside down, resulting in a non-trivial topology where the physical time direction flips across the throat. Path  $(abc)$  is a CTC, with  $(b')$  mirroring  $(b)$ . The shaded area is not a part of the wormhole; it contains physical singularities at  $r = 0$  and  $r = r_*$ .

represent a wormhole throat, and the identification of antipodal points  $(T, X)$  and  $(-T, -X)$  on these lines signifies a *single spacetime event occurring on the throat*. It is important to note that this identification is limited strictly to points on the throat. Points that stay off the throat do *not* enjoy this privilege; they correspond to independent events occurring on separate spacetime sheets. (Note: Our procedure contrasts with historical maneuvers known as “elliptic/antipodal identification” [33–40]. In particular, when dealing with the regular KS diagram of a Schwarzschild spacetime, Rindler [33] assigned each antipodal pair to the same event unrestrictedly, whereas Popławski and other authors [35–40] applied such an assignment to antipodal points that lie on the Schwarzschild horizon.)

In Fig. 2, the trajectory  $A \rightarrow B \equiv C \rightarrow D \rightarrow E \equiv F \rightarrow A$  constitutes a closed timelike loop. Note that Points B and C, as well as Points E and F, are antipodal on the throat and, therefore, identical. The segments between these points can freely take any form as long as they reside within the lightcones. One key feature is that while the segment  $F \rightarrow A \rightarrow B$  progresses in an increasing order of the ‘time’ coordinate  $t$ , the other segment  $C \rightarrow D \rightarrow E$  advances in a *decreasing* order of  $t$ . (Note: the proper time  $\tau$  *increases* along  $C \rightarrow D \rightarrow E$ . Essentially, the wormhole throat serves as a gateway to another *time-reversed* world by connecting two sheets with *opposing* physical time flows.

Akin to the DP space which incurs an alteration of spacetime topology, the  $\zeta$ -KS diagram acquires a non-trivial topology. However, rather than relying on abstract manipulation as in the DP space, the change in topology for our  $\zeta$ -KS diagram takes place spontaneously, driven by the inherent higher-derivative nature of the  $\mathcal{R}^2$  theory. The pertinent sections of the Penrose diagram are shown in Fig. 3, with explanations provided in its caption. Owing to the antipodality, the left wedge must be flipped upside down to facilitate the gluing of the two thick red lines in forming an MTB wormhole.

It is worth noting that the opposite time flows for physical processes in Quadrants (I) and (III) have been known since

the conception of the KS diagram in the 1960s. Yet, this fact has often been overlooked in wormhole studies, most likely because of the prevalent use of embedding diagrams, which are a standard technique for visualizing wormholes. Embedding diagrams obscure a fundamental feature, as they suggest ‘gluing’ the two sheets along the two angular directions, namely the polar and azimuth angles ( $\theta$  and  $\varphi$ ), at the minimal areal radius. However, in an MTB wormhole, the ‘gluing’ actually occurs in *three* directions – the angular ones ( $\theta$  and  $\varphi$ ) *and* the time direction ( $t$ ). This only becomes evident with the explicit use of the  $\zeta$ -KS diagram. In Fig. 2, one of the thick red lines needs to be flipped upside down, and then the two said lines get glued in their *entirety*, viz. along the time direction as well, besides  $\theta$  and  $\varphi$ .

The portal connecting two time-reversed sheets is ubiquitous not only in pure  $\mathcal{R}^2$  gravity but also in Brans–Dicke and scalar–tensor theories, as they share a similar KS diagram [32]. It is intuitive to expect that time-reversed portals are a common feature among wormholes in general. It is important to emphasize that the violation of the WEC plays a crucial role in forming wormholes in scalar–tensor gravity. In this situation, whereas the (local) geometry of spacetime remains Riemannian, *its (global) topology has been drastically altered*, which is a prerequisite for the emergence of wormholes and CTCs. This fulfills the vision of Deutsch–Politzer and Krasnikov mentioned in the Introduction [20–23].

We will now present three corollaries arising from the existence of CTCs in the MTB wormhole.

*Corollary #1: Perception of time reversal via light signal exchange*—The upper panel of Fig. 4 exhibits the case. Consider a Traveler in the left sheet emitting light signals into the wormhole in the order  $A, B, C$ , and  $D$ ; the light signals emerge into the right mouth and continue on their respective null paths. Note that on the throat, each antipodal pair corresponds to a single event, viz.  $A_1 \equiv A_2, B_1 \equiv B_2, C_1 \equiv C_2$ , and  $D_1 \equiv D_2$ . An Observer residing in the right sheet receives light signals in a *reversed* order,  $D', C', B',$  then  $A'$ , however. Therefore, from the Observer’s perspective, the Traveler appears to move backward in time. The perception is mutually symmetric: the Traveler would perceive the Observer as moving backward with respect to the Traveler.

*Corollary #2: Backward flow of information against time*—In the lower panel of Fig. 4, we depict another closely related effect. Consider a Traveler in the left sheet. At point  $A$ , he emits a light signal that enters the wormhole at  $A_1$  and emerges at  $A_2$  (note their antipodal nature). The Traveler then passes into the wormhole and escapes to the right sheet. Choosing a trajectory such that at point  $A'$  (where he crosses paths with the original light signal), he deflects the light signal back into the wormhole (e.g., using a mirror). The chosen path bends ‘outward’ to the right, delaying the reflection event. The deflected light signal at  $A'$  re-enters the throat at  $A'_1$  and re-emerges at  $A'_2$  (again, note their antipodal nature). Finally, the light signal arrives at point  $A''$ , preceding the emission event  $A$ .

*Corollary #3: Bidirectional time flow on the throat*—A Traveler sitting precisely on the throat could proceed either forward into the right sheet or backward into the left sheet. If choosing to reside on the throat, both directions of time are admissible for him.

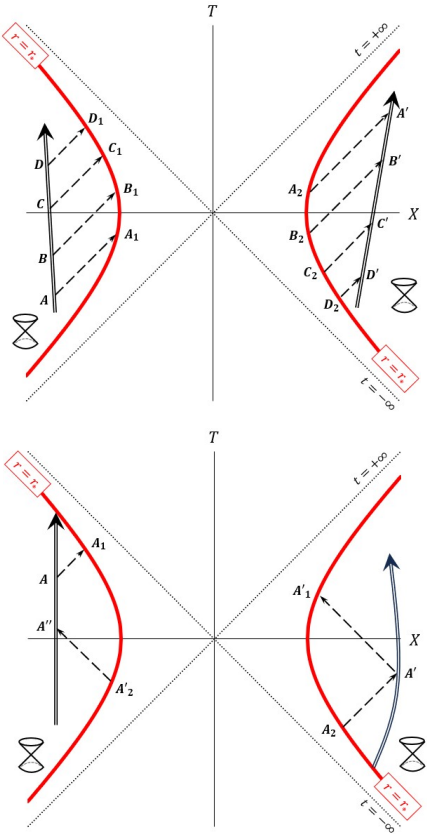


Figure 4. Illustration of Corollaries #1 and #2. Upper panel: Traveler in the left sheet regularly sends light signals to Observer in the right sheet (Note:  $A_1 \equiv A_2$ ,  $B_1 \equiv B_2$  and so on.) The order of arrival for light signals is *reversed*. Lower panel: Traveler at  $A$  sends out a light signal, then crosses through the throat. Later on, Traveler while passing by  $A'$  deflects the light signal back; the light signal arrives at  $A''$  which precedes its emission event  $A$ . (Note:  $A_1 \equiv A_2$  and  $A'_1 \equiv A'_2$ .)

*Prevention of free will to act on foreknowledge?*—There seems to be no inherent principle forbidding microscopic objects from “exploiting foreknowledge to their advantage”. Inanimate objects lack free will to alter history, such as murdering their younger selves or preemptively securing the winning lottery tickets. A timelike path involving ‘time travel’ for microscopic particles would pose no such threat and should be allowed to contribute in the Feynman sum of transition amplitudes for these particles, as we will formulate shortly. The implications of foreknowledge on macroscopic animate objects constitute a subject of ongoing debate and deliberation, nevertheless [2, 6, 7, 9–19]. We venture one view: macroscopic objects might undergo a strong decoherence process upon passing through the wormhole throat. If violent enough, the decoherence could erase, for instance, the mental state of an intrepid traveler crossing the throat. For example, in Corollary #2 above, memory erasure could derail the Traveler from carrying out his plan to deflect the light signal at  $A'$ , thus thwarting its ‘early’ arrival at  $A''$ . This decoherence-based reasoning could be applicable to macroscopic objects in general, such as an unmanned spaceship pre-programmed to traverse to  $A'$  to deflect the light signal. The decoherence might erase its computer program and sabotage its planned itinerary.

Interestingly, in parallel with our decoherence-based proposal that forbids the use of foreknowledge as discussed herein, a more recent article has suggested a mechanism to “erase” the memory of animate travelers, potentially avoiding time-travel paradoxes [41].

*Quantum effects induced by time-reversed paths*—Using metric (2), we can cast the proper time between two events  $A$  and  $B$ ,  $\tau_{AB} = \int_A^B d\tau$ , as a functional of  $\vec{r}(t) := \{r(t), \theta(t), \varphi(t)\}$ , given by

$$\tau_{AB} = \int_{t_A}^{t_B} dt \left(1 - \frac{1}{r}\right)^{\frac{\tilde{k}-1}{2\zeta}} \times \left[ \left(1 - \frac{1}{r}\right)^{\frac{2}{\zeta}} - \left(\dot{r}^2 + \left(1 - \frac{1}{r}\right)r^2(\dot{\theta}^2 + \sin^2 \theta \dot{\varphi}^2)\right) \right]^{\frac{1}{2}} \quad (5)$$

with the overdot indicating a derivative with respect to  $t$ . Denoting  $z := 1 - r_s/r \in [r_*, 1)$  with  $r_* := 1 - r_s/r_*$  and  $r_*$  given in Eq. (4) specifying the location of the throat, Eq. (5) yields

$$\tau_{AB} = \int_{t_A}^{t_B} \frac{dt}{(1-z)^2} z^{\frac{\tilde{k}-1}{2\zeta}} \left[ z^{\frac{2}{\zeta}} (1-z)^4 - \dot{z}^2 - z(1-z)^2(\dot{\theta}^2 + \sin^2 \theta \dot{\varphi}^2) \right]^{\frac{1}{2}} \quad (6)$$

The geodesics in the plane  $\theta = \pi/2$ , obtained by extremizing the functional (6), satisfies the following equations, with  $l$  and  $\mathcal{E}$  being two constants of motion:

$$\dot{z} = (1-z)^2 z^{\frac{1}{\zeta}} \frac{1}{\mathcal{E}} \sqrt{\mathcal{E}^2 - (1-z)^2 z^{\frac{2-\zeta}{\zeta}} l^2 - z^{\frac{\tilde{k}+1}{\zeta}}} \quad (7)$$

$$\dot{\varphi} = (1-z)^2 z^{\frac{2}{\zeta}-1} \frac{l}{\mathcal{E}} \quad (8)$$

In the large  $\mathcal{E}$  limit, Eqs. (7)–(8) are integrable to yield  $t - t_0 = \frac{1}{1-1/\zeta} z^{1-1/\zeta} {}_2F_1(2, 1-1/\zeta; 2-1/\zeta; z)$  and  $\varphi = \text{const}$ , corresponding to a pure radial motion.

Consider now a pair of starting and end points  $A$  and  $B$  situated in the right sheet. Note that Eq. (6) has been defined for a *single-valued* function  $z(t)$  that connects  $A$  with  $B$  while staying above the line  $z = z_*$ . This scenario is depicted in the upper left plot in Fig. 5, showing 3 paths with no crossing into the left sheet (the boundary of which is the horizontal axis  $t$ , representing  $z = z_*$ ).

When a path crosses the wormhole throat and ventures into the left sheet, the respective segment in the left sheet has a reversed time direction, however. This can conveniently be superimposed in the same  $(t, z)$  plane except with an orientation against the direction of  $t$ . Other plots in Fig. 5 showcase the once-time-reversed and twice-time-reversed paths. Given the additive nature of proper time, it is straightforward to see, for example, that for the once-time-reversed path:  $\tau_{AA_1A_2B} = \tau_{AA_1} + \tau_{A_1A_2} + \tau_{A_2B}$ .

The transition amplitude of a particle of mass  $m$ , as usual, is given by a Feynman sum,  $K(\vec{z}_B, \vec{z}_A; t_B - t_A) \simeq \int \mathcal{D}\vec{z}(t) \exp(-im\tau_{AB}(\vec{z}(t)))$ . Note that in the absence of a wormhole throat, all paths that contribute to the Feynman sum must run forward in time; this means that

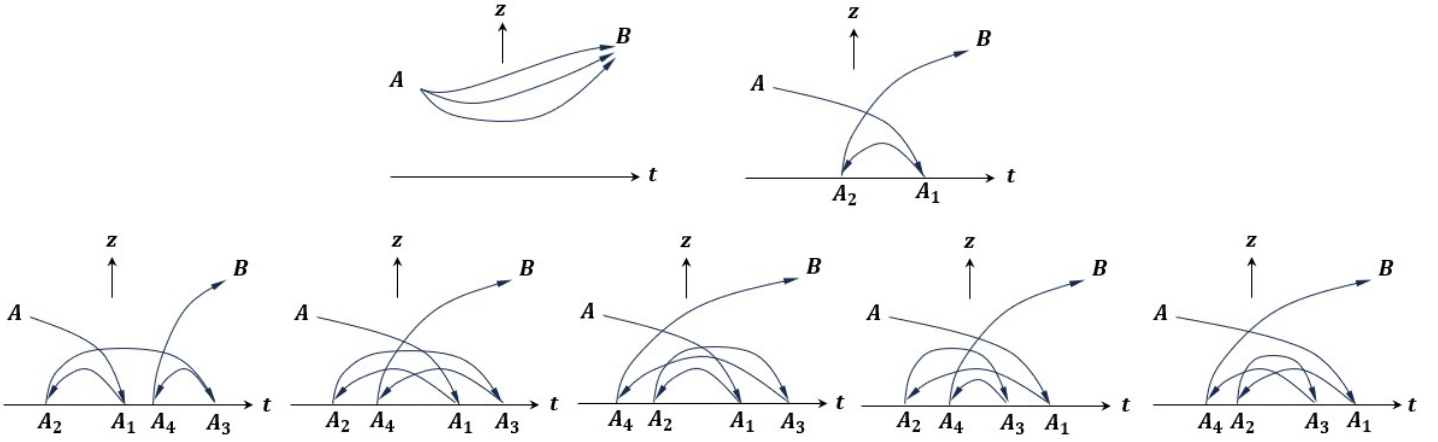


Figure 5. Different transition paths from Event A to Event B (both located in the right sheet of the wormhole). In the upper row, 3 paths exhibit no crossing into the left sheet, while another path involves a single crossing into the left sheet and subsequent return. The lower row presents 5 admissible arrangements for paths with two crossings into the left sheet and twice-returning. In all cases, traversal in the left sheet is depicted by a segment oriented against the direction of  $t$ , meaning that a time-reversed path entails a *multi-valued* function  $z(t)$ .

the function  $z(t)$  is single-valued. However, when facilitated by a wormhole, a time-reversed path would make  $z(t)$  a *multi-valued* function, as is evident from Fig. 5. The contribution of time-reversed paths into the Feynman sum is thus a novel non-trivial aspect. Moreover, in the proximity of a throat, timelike paths with multiple time reversals could proliferate and significantly—if not fundamentally—alter the transition amplitude of free particles. This intuitive possibility underscores the importance of the decoherence process discussed in relation to safeguarding causality for macroscopic objects. We leave this arena open for future exploration.

Consider now the evolution of a system, for simplicity, restricted within the plane  $\theta = \pi/2$ . The action of an object of mass  $m$  is  $S = -m \int d\tau$ . By virtue of the definition of the Lagrangian via  $S = \int dt L$ , and from Eq. (6), we deduce the following Lagrangian

$$L := -\frac{m z^{\frac{k-1}{2\zeta}}}{(1-z)^2} \left[ z^{\frac{2}{\zeta}}(1-z)^4 - \dot{z}^2 - z(1-z)^2 \dot{\varphi}^2 \right]^{\frac{1}{2}} \quad (9)$$

and, via the generalized momenta  $p_z := \frac{\delta L}{\delta \dot{z}}$  and  $p_\varphi := \frac{\delta L}{\delta \dot{\varphi}}$ , the associated Hamiltonian is given by

$$H = p_z \dot{z} + p_\varphi \dot{\varphi} - L \quad (10)$$

$$= z^{\frac{1}{\zeta}} \sqrt{(1-z)^4 p_z^2 + z^{-1}(1-z)^2 p_\varphi^2 + m^2 z^{\frac{k-1}{\zeta}}} \quad (11)$$

with  $p_\varphi$  and  $H$  being two constants of motion.

Hamiltonians are known to be suitable for the Heisenberg picture when describing the evolution of free particles and for the interaction picture when building the Feynman rules for quantum field theories. Despite the apparent asymmetric treatment of the time direction (versus the spatial ones) by the Hamiltonian, relativistic covariance is duly restored in the final results [42]. In

the context of an MTB wormhole, where the background metric is static and inert, the Hamiltonian could find utility. As a by-product, the form of the Hamiltonian in Eq. (11) is also evocative of Dirac's historical approach towards the (relativistic) Dirac equation in 1927. Starting from the energy-momentum relation  $E^2 = p^2 + m^2$  and requiring the field equation for the electron to be first-order, Dirac conceived the spinors and the associated Clifford algebra for the Dirac gamma matrices in Minkowski spacetime. Notwithstanding the tetrad formalism, Expression (11) suggests pathways for an alternative and convenient representation of Dirac's spinor fields in the presence of an MTB wormhole. The Clifford algebra may be adapted to conform with the altered energy-momentum relation, obtained by 'squaring' Eq. (11):

$$z^{-\frac{2}{\zeta}} E^2 = (1-z)^4 p_z^2 + z^{-1}(1-z)^2 p_\varphi^2 + m^2 z^{\frac{k-1}{\zeta}} \quad (12)$$

Lastly, the time-reversed information flows across a wormhole, as demonstrated in Corollary #2, could potentially impact the unitarity of the evolution operator and the time-ordered product in the interaction picture. These intriguing prospects warrant in-depth exploration.

As our final remark, although CTCs appear to be an inevitable feature of wormholes constructed from scalar-tensor gravity, the decoherence effect discussed herein, together with the "memory eraser" mechanism independently proposed in [41], could prevent paradoxes related to time travel of animate objects, thereby rescuing scalar-tensor gravity from inherent inconsistencies.

*Acknowledgments*—We wish to thank the anonymous referee for their constructive and valuable comments which helped improve the quality of our Letter. HKN thanks Tiberiu Harko, Mustapha Azreg-Aïnou,

Luis A. Correa-Borbonet, Lorenzo Gavassino, and Nicholas Buchdahl. FSNL acknowledges support from the Fundação para a Ciência e a Tecnologia (FCT)

Scientific Employment Stimulus contract with reference CEECINST/00032/2018, and funding from the research grants UIDB/04434/2020 and UIDP/04434/2020.

---

[1] W. J. van Stockum, *The Gravitational Field of a Distribution of Particles Rotating about an Axis of Symmetry*, Proc. Roy. Soc. Edinburgh **57**, 135 (1938)

[2] K. Gödel, *An Example of a New Type of Cosmological Solution of Einstein's Field Equations of Gravitation*, Rev. Mod. Phys. **21**, 447 (1949)

[3] M. S. Morris and K. S. Thorne, *Wormholes in spacetime and their for interstellar travel: A tool for teaching general relativity*, Am. J. Phys. **56**, 5 (1988)

[4] M. S. Morris, K. S. Thorne, and U. Yurtsever, *Wormholes, Time Machines, and the Weak Energy Condition*, Phys. Rev. Lett. **61**, 1446 (1988)

[5] V. P. Frolov and I. D. Novikov, *Physical effects in wormholes and time machines*, Phys. Rev. D **42**, 1057 (1990)

[6] I. D. Novikov, *Time machine and self-consistent evolution in problems with self-interaction*, Phys. Rev. D **45**, 1989 (1992)

[7] F. G. Echeverria, G. Klinkhammer, and K. S. Thorne, *Billiard Balls in Wormhole Spacetimes with Closed Timelike Curves: Classical Theory*, Phys. Rev. D **44**, 1077 (1991)

[8] M. Visser, *Lorentzian Wormholes: From Einstein to Hawking*, Springer-Verlag 1996

[9] F. J. Tipler, *Causality violation in asymptotically flat space-times*, Phys. Rev. Lett. **37**, 879 (1976)

[10] J. L. Friedman, M. S. Morris, I. D. Novikov, F. Echeverria, G. Klinkhammer, K. S. Thorne, and U. Yurtsever, *Cauchy problem in spacetimes with closed timelike curves*, Phys. Rev. D **42**, 1915 (1990)

[11] A. Ori, *Must time machine construction violate the weak energy condition?*, Phys. Rev. Lett. **71**, 2517 (1993)

[12] A. Ori, *A class of time-machine solutions with a compact vacuum core*, Phys. Rev. Lett. **95**, 021101 (2005), arXiv:gr-qc/0503077

[13] M. Alcubierre, *The warp drive: Hyperfast travel within general relativity*, Class. Quant. Grav. **11**, L73 (1994), arXiv:gr-qc/0009013

[14] M. Alcubierre and F. S. N. Lobo, *Wormholes, Warp Drives and Energy Conditions*, Fundam. Theor. Phys. **189**, 257-279 (2017), Springer 2017.

[15] A. E. Everett, *Warp drive and causality*, Phys. Rev. D **53**, 7365 (1996)

[16] J. Pfarr, *Time travel in Gödel's space*, Gen. Rel. Grav. **13**, 1073 (1981)

[17] F. de Felice and M. Calvani, *Time machine and geodesic motion in Kerr metric*, Gen. Rel. Grav. **9**, 155 (1978)

[18] J. R. Gott, *Closed Timelike Curves Produced by Pairs of Moving Cosmic Strings: Exact Solutions*, Phys. Rev. Lett. **66**, 1126 (1991)

[19] S. W. Hawking, *Chronology protection conjecture*, Phys. Rev. D **46**, 603 (1992)

[20] D. Deutsch, *Quantum mechanics near closed timelike lines*, Phys. Rev. D **44**, 3197 (1991)

[21] H. D. Politzer, *Simple quantum systems in spacetimes with closed timelike curves*, Phys. Rev. D **46**, 4470 (1992)

[22] S. V. Krasnikov, *A singularity-free WEC-respecting time machine*, Class. Quant. Grav. **15**, 997 (1998)

[23] S. V. Krasnikov, *Topology Change without any Pathology*, Gen. Rel. Grav. **27**, 529 (1995)

[24] T. Harko, F. S. N. Lobo, M. K. Mak, and S. V. Sushkov, *Modified-gravity wormholes without exotic matter*, Phys. Rev. D **87**, 067504 (2013), arXiv:1301.6878 [gr-qc]

[25] K. A. Bronnikov, M. V. Skvortsova, and A. A. Starobinsky, *Notes on wormhole existence in scalar-tensor and  $F(R)$  gravity*, Grav. Cosmol. **16**, 216 (2010), arXiv:1005.3262 [gr-qc]

[26] H. K. Nguyen, *Beyond Schwarzschild-de Sitter spacetimes: II. An exact non-Schwarzschild metric in pure  $R^2$  gravity and new anomalous properties of  $R^2$  spacetimes*, Phys. Rev. D **107**, 104008 (2023), arXiv:2211.03542 [gr-qc]

[27] H. K. Nguyen, *Beyond Schwarzschild-de Sitter spacetimes: A new exhaustive class of metrics inspired by Buchdahl for pure  $R^2$  gravity in a compact form*, Phys. Rev. D **106**, 104004 (2022), arXiv:2211.01769 [gr-qc]

[28] H. K. Nguyen, *Buchdahl-inspired spacetimes and wormholes: Unearthing Hans Buchdahl's other 'hidden' treasure trove*, Int. J. Mod. Phys. D (2023) 2342007, arXiv:2305.08163 [gr-qc]

[29] H. A. Buchdahl, *On the Gravitational Field Equations Arising from the Square of the Gaussian Curvature*, Nuovo Cimento **23**, 141 (1962), link.springer.com/article/10.1007/BF02733549

[30] H. K. Nguyen and M. Azreg-Aïnou, *Traversable Morris-Thorne-Buchdahl wormholes in quadratic gravity*, Eur. Phys. J. C **83**, 626 (2023), arXiv:2305.04321 [gr-qc]

[31] H. K. Nguyen and F. S. N. Lobo, *Closed Timelike Curves induced by a Buchdahl-inspired vacuum spacetime in  $R^2$  gravity*, Universe **9**, 467 (2023), arXiv:2310.19829 [gr-qc]

[32] H. K. Nguyen and M. Azreg-Aïnou, *Revisiting Weak Energy Condition and wormholes in Brans-Dicke gravity*, arXiv:2305.15450 [gr-qc]

[33] W. Rindler, *Elliptic Kruskal-Schwarzschild space*, Phys. Rev. Lett. **15**, 1001 (1965)

[34] E. Schrödinger, *Expanding Universes*, Cambridge University Press 1957, Sec. 3

[35] N. J. Popławski, *Radial motion motion into an Einstein-Rosen bridge*, Phys. Lett. B **687**, 110 (2010), arXiv:0902.1994 [gr-qc]

[36] N. Sánchez, *Quantum field theory and the "elliptic interpretation" of de Sitter spacetime*, Nucl. Phys. B **294**, 1111 (1987)

[37] N. Sánchez and B. F. Whiting, *Quantum field theory and the antipodal identification of black-holes*, Nucl. Phys. B **283**, 605 (1987)

[38] G. Domenech, M. L. Levinas, and N. G. Sanchez, *Quantum field theory and the antipodal identification of space-time*, Int. J. Mod. Phys. A **3**, 2567 (1988)

[39] N. A. Strauss, B. F. Whiting, and A. T. Franzen, *Classical Tools for Antipodal Identification in Reissner-Nordström Spacetime*, Class. Quant. Grav. **37**, 185006 (2020), arXiv:2002.02501 [gr-qc]

- [40] G. 't Hooft, *Black Hole Unitarity and Antipodal Entanglement*, Found. Phys. **46**, 1185 (2016), [arXiv:1601.03447 \[gr-qc\]](https://arxiv.org/abs/1601.03447)
- [41] L. Gavassino, *Life on a closed timelike curve*, [arXiv:2405.18640 \[gr-qc\]](https://arxiv.org/abs/2405.18640)
- [42] J. J. Sakurai, *Advanced Quantum Mechanics*, Addison-Wesley 1967, Chap. 4